Inorganic Chemistry

pubs.acs.org/IC

Article

Alkyl Radical-Free Cu(I) Photocatalytic Cross-Coupling: A Theoretical Study of Anomerically Specific Photocatalyzed Glycosylation of Pyranosyl Bromide

Richard N. Schaugaard, Hien M. Nguyen,* and H. Bernhard Schlegel*

Cite This: https://doi.org/10.1021/acs.inorgchem.1c01038

Read Online

ACCESS | Metrics & More | Article Recommendations | Supporting Information

ABSTRACT: Previously, we reported a visible light-activated Cu(I) photocatalyst capable of facilitating C−O bond formation of glycosyl bromides and aliphatic alcohols with a high degree of diastereoselectivity. This catalyst functions equally well in the presence of radical traps, suggesting an entirely inner sphere mechanism atypical for heteroleptic Cu photocatalysis. Further, experimental estimates put the chromophore reducing power at −1.30 V vs Ag/AgCl. This is much more positive than the ∼−2.0 V vs Ag/AgCl onset observed for irreversible reduction of glycosyl bromides in our experiments. Theoretical investigations were undertaken to explain the function of the catalyst. Outer sphere electron transfer from a chromophore to substrate was discounted based on thermodynamics and electron transfer barriers determined by Marcus theory and non-equilibrium solvation calculations. Unactivated and activated chromophores were found to disproportionate to Cu(0) and Cu(II) species. The resulting Cu(0) species undergoes oxidative addition with a glycosyl bromide generating a Cu(II) species. Addition of a nucleophilic alcohol and oxidation of the Cu(II) species to Cu(III) result in rapid reductive elimination forming products and resetting the catalytic cycle.

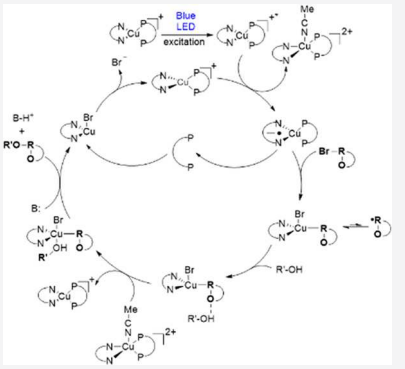

INTRODUCTION

The practical use of copper to facilitate cross-coupling of organic substrates has a history stretching back 100 years with Ullmann and Goldberg's development of their namesake reactions.[1−4] However, these reactions have fallen out of favor in recent times due to their limited substrate scope and the relatively harsh conditions required by thermal activation of the catalysts, typically ∼200 °C. Under such conditions, even regioselectivity is difficult to achieve, which led to the development of catalysts based on less earth-abundant metals, such as palladium, which came to dominate cross-coupling catalysis.[5−10] However, the interest in using copper for cross-coupling did not wane completely owing to the relative abundance and the reduced toxicity of copper compared to the second and third row transition metal catalysts.[11] The efficient construction of well-defined, biologically relevant oligosaccharides has been a major focus in carbohydrate synthesis. Adoption of copper to stereoselectivity connects pyranosyl electrophiles to carbohydrate hydroxyl nucleophiles to generate oligosaccharides is especially appealing and has been one of our primary motivations for developing this chemistry.

The adoption of Cu(I) complexes as a cross-coupling catalyst is not without major challenges. The limited substrate scope of thermally activated Cu(I) cross-couplings has been especially restricting, with C(sp^2) couplings being common but C(sp^3) activations being much less frequent. Advancements in ligand design and the use of non-nucleophilic bases pioneered by Buchwald and Hartwig have allowed C(sp^2) coupling reactions to proceed under milder conditions than older Ullmann-type reactions.[12−14] However, with the exception of particularly favorable substrates such as aryl boronic acids,[15,16] the temperatures required for such reactions are typically still in a range of 60−160 °C for C(sp^2) cross-couplings.[12,17] Couplings involving alkyl halides, a common starting material for the C−O glycosidic linkages that connect monosaccharide sugar units to form oligosaccharides, are unknown to the body of thermally activated Cu cross-coupling literature. An understanding of the mechanistic details of copper-catalyzed cross-couplings is needed to expand the potential of this process.

In 2010, insights into the mechanism of copper-catalyzed cross-coupling of iodobenzene derivatives with aliphatic alcohols and primary amines were achieved by detailed computational investigations from Buchwald and Houk (Figure 1).[18] Among the pathways explored in that work were an oxidative addition/reductive elimination cycle, single

Received: April 4, 2021

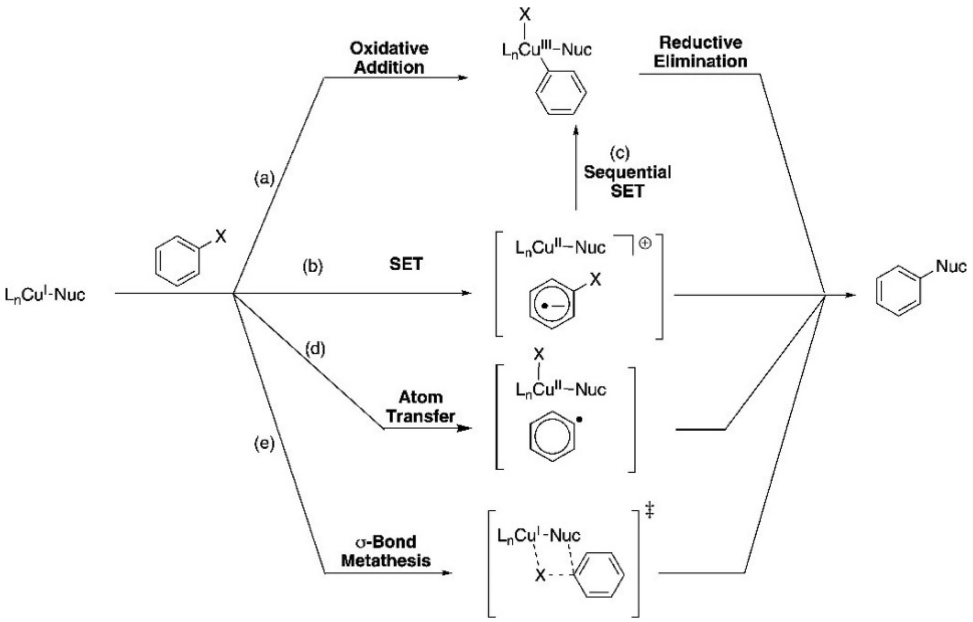

Figure 1. Possible mechanisms for copper-catalyzed cross-coupling reactions.[18] Reproduced from ref 18. Copyright 2010 American Chemical Society.

electron transfer (SET), and iodine atom transfer (IAT) (Figure 1). Oxidative addition was consistently disfavored by ~20 kcal/mol relative to SET and IAT, possibly due to the instability of the aryl-Cu(III) intermediates generated by that process. Both IAT and SET avoid the issues with Cu(III) by generating a Cu(II) intermediate and a reactive radical species. The understanding from this study also points to a new method for enabling Cu cross-coupling without the need for thermal conditions: SET by a Cu chromophore.

Photoactive copper species have been known as SET donors since at least 1977 with McMillin et al.'s development of a bis-phenanthroline-based Cu photocatalyst.[19] In 1987, Sauvage and Kern improved the excited state lifetimes of these systems by using two bulky phenanthroline-type ligands to enforce rigidity of the primary coordination sphere and prevent excited state decay by intersystem crossing.[20] Sauvage and Kern's enhancements allowed for SET to benzyl bromides and subsequent homo coupling of these substrates through the benzylic position (Figure 2a). Building on this further, the use of rigid heteroleptic Cu(I) complexes leads to increased excited state lifetimes and greater reducing power of activated Cu(I) chromophores.[11] However, it was not until 2012 that Fu et al. demonstrated that heteroleptic Cu(I) complexes were capable of performing cross-coupling reactions with a substrate scope that was beyond that of thermally activated Cu complexes (Figure 2b).[21−24] The viability of alkyl halides as electrophilic coupling partners was of particular interest to us as this pointed to a new method for performing glycosylation reactions.

We recently have identified a chromophore capable of activating C(sp^3)−Br bonds of a sugar substrate for coupling with an alkyl alcohol (Scheme 1a).[25] As with many other heteroleptic Cu(I) complexes, it is activated by a visible light source, resulting in cleavage of an organic halide bond and subsequent stereospecific coupling of a nucleophile to the position formerly occupied by the halide. Importantly, the system functions equally well in the presence and absence of classic radical traps such as TEMPO (Scheme 1c) and

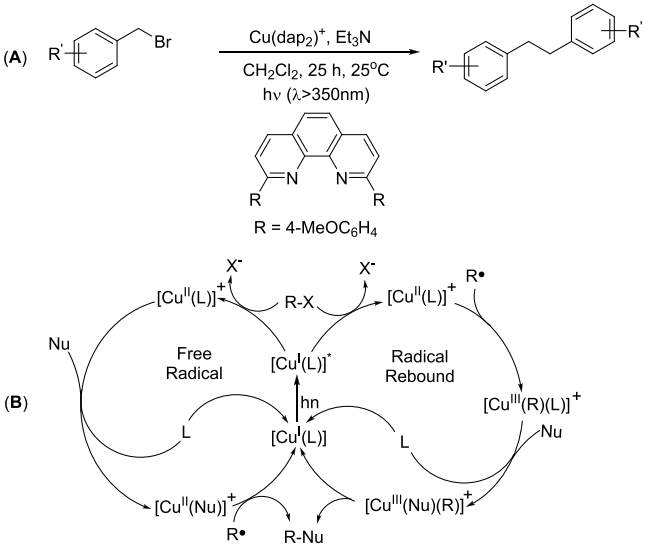

Figure 2. (A) Sauvage and Kern's $Cu(dap_2)^{+*}$ initiated homo coupling of substituted benzylic bromides. (B) Free-radical mechanism reported by Fu et al. (left) and the radical rebound mechanism reported by Reiser et al. (right) for cross-coupling by homoleptic Cu chromophores.

intramolecular alkenes vicinal to the halide (Scheme 1c). These results suggest that there is no long-lived organic radical intermediate in our reaction. Further, estimation of the chromophore's reducing potential by UV−Vis excitation/emission and electrochemical oxidation put the reducing power at −1.30 V vs Ag/AgCl (Figure 5) compared to the ~−2.0 V vs Ag/AgCl that we observed in electrochemical experiments to measure onset voltage for irreversible reduction of a glycosyl bromide (Figure 6). Since the reducing power of the chromophore is well below what is needed to generate a glycosyl radical through an outer sphere mechanism, our catalyst does not seem to follow the same mechanistic pathway predicted by Buchwald and Houk. The mechanism of our

https://doi.org/10.1021/acs.inorgchem.1c01038
Inorg. Chem. XXXX, XXX, XXX−XXX

Scheme 1. Visible Light-Mediated Photoinduced Copper-Catalyzed Cross-Coupling of Pyranosyl Bromide with Aliphatic Alcohol (A); Presence of a C2-Bound Alkene Group (B) and (C) Radical Traps such as TEMPO Do Not Affect Yield or Selectivity of the Reaction.[25]

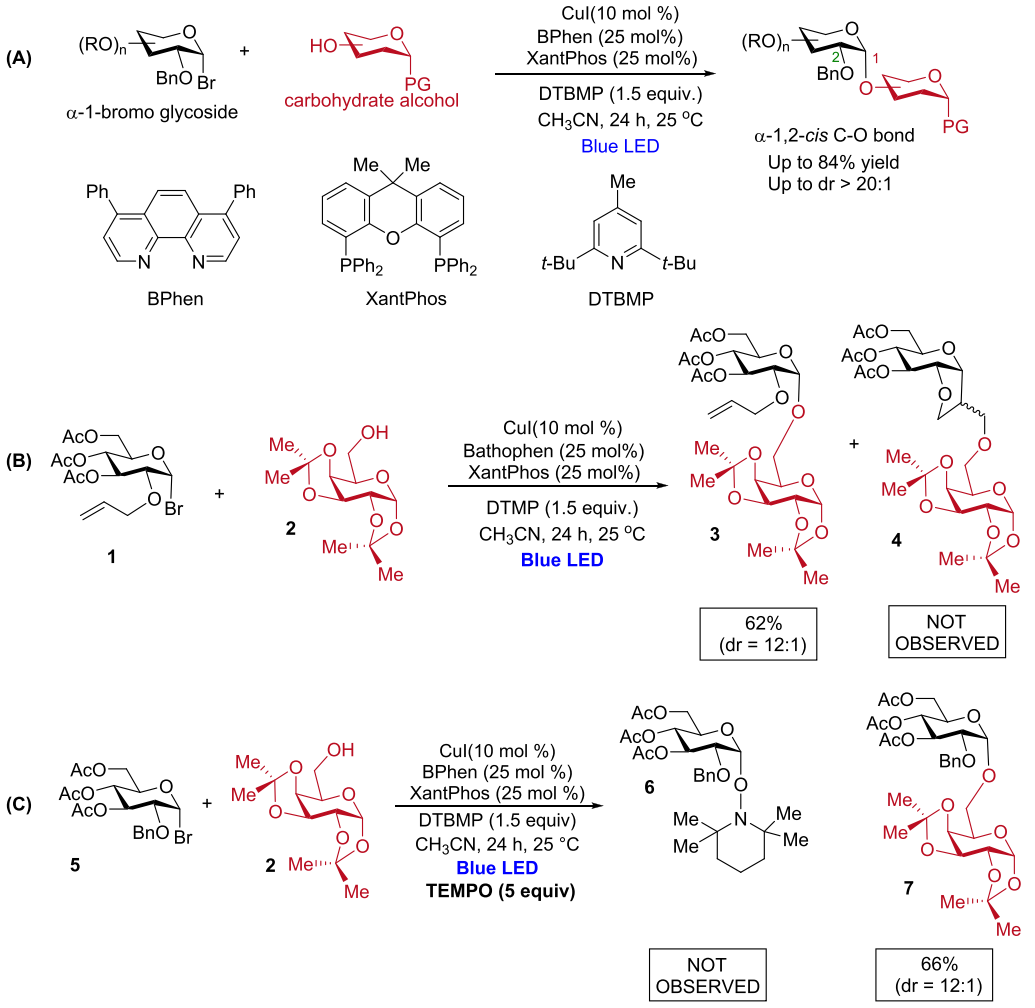

Reproduced from ref 25. Copyright 2020 American Chemical Society.

catalyst is certainly an outlier since experimental results from heteroleptic Cu photocatalysts have largely been consistent with Buchwald and Houk's mechanism as they are susceptible to the presence of a radical trap, which intercepts the critical radical intermediate preventing the desired cross-coupling reaction.[21−24,26,27]

In light of these unusual experimental results, we considered that our reaction may proceed through an inner sphere mechanism. Reiser et al. have reported an inner sphere for some Cu(I) chromophore systems, but in that case, a radical intermediate can be trapped by TEMPO, consistent with a radical rebound or sequential SET reaction (Figure 1c).[26-27] Based on our experimental results demonstrating a mechanistic imperviousness to TEMPO, an oxidative addition step is possible and certainly merits investigation. The other major mechanistic problem for our system is that the experimentally estimated reducing power of our chromophore appears to be insufficient to activate bromoglucoside **1**. Nevertheless, the reaction proceeds to products. This issue has already been resolved by Evano and co-workers who have demonstrated that a single electron donor can be used to augment the reducing power of an otherwise insufficiently reducing chromophore (Figure 3).[28] As such, we incorporated this idea into our mechanism.

In this paper, the identity of the Cu-containing species in solution under equilibrium conditions was investigated to determine the likely distribution of Cu species present in the reaction mixture. The electronic and thermodynamic nature of the Cu excited state was also investigated with an emphasis on

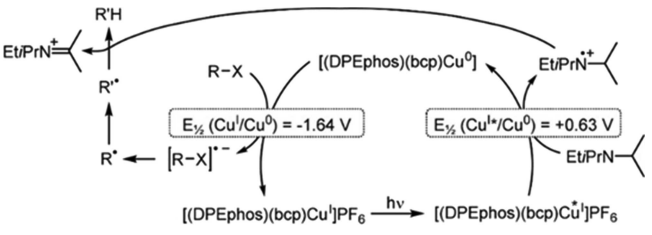

Figure 3. Novel mechanism reported by Evano and co-workers for enhancing the reducing power of a Cu chromophore by reduction of a Cu(I)* species to Cu(0) by a *ter*-amine sacrificial electron and hydrogen atom donor. The reducing power of the Cu complex in this case is enhanced 0.63 V by the sacrificial electron donor. Reproduced from ref 28. Copyright 2017 American Chemical Society.

https://doi.org/10.1021/acs.inorgchem.1c01038
Inorg. Chem. XXXX, XXX, XXX−XXX

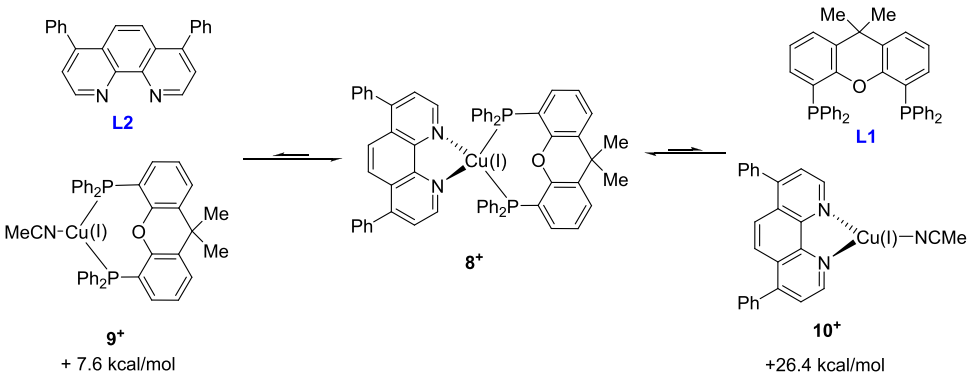

Figure 4. Calculated relative stability of copper species 8^+, 9^+, and 10^+.

understanding the reducing power of this species compared to the redox potentials of the ground state species present under reaction conditions. From this study, we determined that the species most likely to be reduced or oxidized by the activated chromophore is the unactivated chromophore via disproportionation, resulting in a Cu(II) species and a formally Cu(0) species. Oxidative addition of a carbohydrate substrate to the Cu center of the formally Cu(0) species was found to be significantly endergonic but accessible under room temperature conditions. A nucleophilic alcohol coordinates to the resulting coordinatively saturated Cu(II)(L)(X)(R) species as an H-bonded adduct. Oxidation to a Cu(III)(L)(X)(R) species precedes incorporation of ROH into the inner coordination sphere followed by rapid and favorable reductive elimination of products.

COMPUTATIONAL METHODS

To better understand our system, computational investigations were undertaken using the B3LYP functional with D3BJ dispersion correction. Geometry optimization was carried out with the def2-SVPP basis set, and energies were calculated with the def2-TZVPP basis set. The SMD model was used to simulate solvation in MeCN. Further details are available in the Supporting Information provided.

RESULTS AND DISCUSSION

Identity of the Solution Phase Cu Species. The Cu(I) chromophore species 8^+ was formed *in situ* by the addition of XantPhos (**L1**) and phenanthroline (**L2**) to CuI in MeCN (Figure 4). The relative energetics of 8^+ and solvato complexes 9^+ and 10^+ were considered to evaluate the possibility of coordinatively unsaturated Cu complexes existing in solution. The dissociation of **L2** from 8^+ to form 9^+ was found to be 7.6 kcal/mol, and the formation of 10^+ was found to be +26.4 kcal/mol. Thus, we conclude that once equilibrium has been reached, it is unlikely that any Cu species besides 8^+ exists in solution in any appreciable concentration. Therefore, in constructing our mechanism, we did not consider contributions from 9^+, 10^+, or any similarly coordinatively unsaturated Cu species. The involvement of homoleptic species was also found to be unlikely, as discussed in the Supporting Information.

Nature of the Chromophore Excited State 8^{+*}. UV–Vis spectroscopy of the chromophore 8^+ detected an absorption at 404 nm and an emission at 630 nm corresponding to the vertical excitation and emission from the metastable relaxed structure, respectively (Figure 4). Electrochemical results put the oxidation of 8^+ at +0.9 V vs Ag/AgCl. The reducing power of 8^{+*} was determined using the energy difference between the ground state and the metastable excited state as well as the oxidation potential of the ground state. This gives a reducing power of −1.3 V vs Ag/AgCl for the excited state (Figure 5).

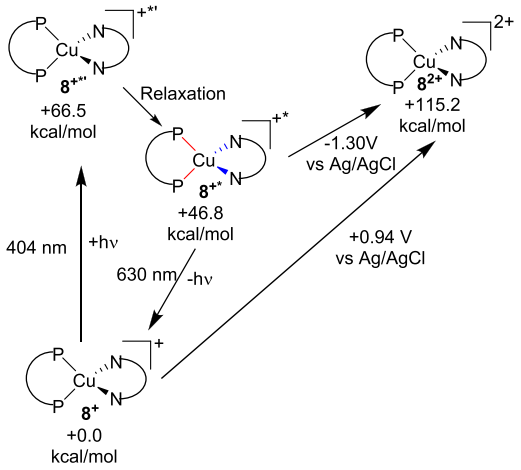

Figure 5. Schematic showing the exitation wavelength of 8^+, the emission wavelength of 8^{+*}, and the estimated reducing power of 8^{+*}.

Computational probes into the excited states of 8^+ are consistent with the experimental results (see above) predicting an absorption at 433 nm, an emission at 611 nm, and a reducing potential of −1.1 V vs Ag/AgCl. The calculated excited state corresponds to a charge transfer state with Cu(I) transferring an electron to the phenanthroline ligand, resulting in a transient Cu(II)(phen^{-1}) species designated as $8^{+*\prime}$ for the vertical excitation species and 8^{+*} for the relaxed structure (Figure 5). The identity of 8^{+*} as a metal to ligand charge transfer was confirmed computationally by the presence spin density on both the Cu center and **L2**. The phenanthroline C–C linkage *ortho* to both N atoms is also shorter for 8^{+*} than 8^+ (1.41 vs 1.47 Å), consistent with occupation of the **L2** LUMO in 8^{+*}. With the energy and electronic structure of the 8^{+*} excited state established, the possible electron transfer reactions of this species can be investigated.

*Electrochemical Studies Comparing Redox Potentials of **12** and 8^{+*}.* Cyclic voltammetry of a pyranosyl bromide **1** demonstrates an irreversible current response initiating at approximately −2.0 V vs Ag/AgCl (Figure 6). This was taken to be the formation of a glycosyl radical **11** since the irreversibility of the reduction wave indicates a significant structural change to the analyte and there were no current

https://doi.org/10.1021/acs.inorgchem.1c01038
Inorg. Chem. XXXX, XXX, XXX–XXX

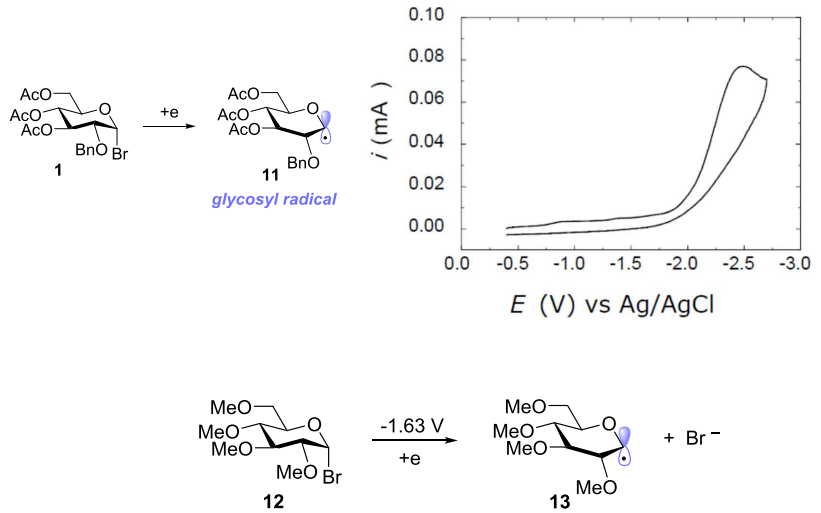

Figure 6. (Top) Cyclic voltamagram of a glycosyl bromide **1** showing the onset formation of glycosyl radical **11** at approximately −2.0 V vs Ag/AgCl.[25] (Bottom) Calculated reduction potential vs Ag/AgCl of **12** forming **13** and Br^-. Reproduced from ref 25. Copyright 2020 American Chemical Society.

responses of a similar magnitude and character at more positive potentials. Since the observed current response is 0.7 V more negative than the estimated reducing power of 8^{+*} (−1.3 V), it is unlikely that the observed coupling can proceed by the direct outer sphere reduction of **12** to form the glycosyl radical **13** as it was for Fu et al.'s systems. This is further supported by the results of radical trapping experiments that failed to detect long-lived free-radical species in contrast to previous studies by Fu et al. and Reiser et al.[21,24,26−30] Since an outer sphere reduction by 8^{+*} seems unlikely by both experimental and computational studies, alternate mechanisms of electron transfer by 8^{+*} and related species were investigated.

Overcoming an Underpowered Reducing Agent by Single Electron Donation. A 2017 paper by Evano and co-workers demonstrated the viability of a Cu(I)/Cu(I)*/Cu(0) cycle for a number of transformations involving organic halides, in contrast to the more commonly reported Cu(I)/Cu(I)*/Cu(II) cycle for the heteroleptic Cu complexes (Figure 7).[28] Rather than reduce the substrate directly, a Cu(I)/Cu(I)*/Cu(0) cycle sees the photoactivated Cu(I)* reduced to a formally Cu(0) species by a single electron donor before reducing the substrate and regenerating the Cu(I) ground state species. In essence, the oxidizing power of the Cu(I)* species

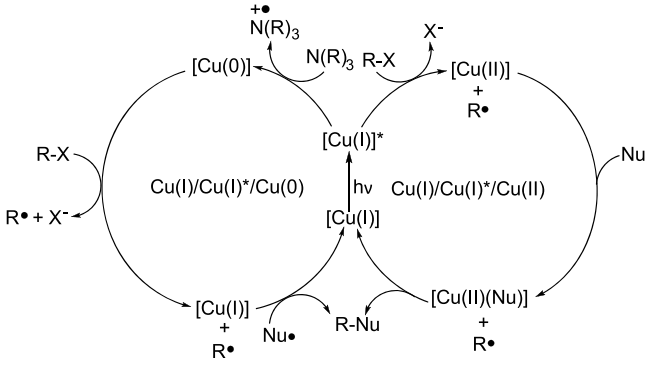

Figure 7. Comparison of Evano and co-workers' Cu(I)/Cu(I)*/Cu(0) cycle mechanism (left) and a typical Cu(I)/Cu(I)*/Cu(II) mechanism (right) for R-X/Nu coupling.

is used to generate a more powerful Cu(0) reductant. The chromophore frontier orbital involved in the outer electron transfer is the lowest lying phenanthroline **L2** π^* for both the Cu(I)* and Cu(0) species. However, the decreased Lewis acidity of the Cu center in the Cu(0) species compared to Cu(I)* leads to a more favorable reduction potential for the Cu(0) species.

In line with the work of Evano and co-workers, we considered the possibility of a serendipitous single electron donor amplifying the reducing power of 8^{+*}. The species xanthphos **L1**, phenanthroline **L2**, 8^+, and DTBMP were evaluated to determine if they were competent to donate an electron to 8^{+*}. These are the species most likely to be oxidized that have significant concentrations in the reaction mixture. Reduction of **L1** and **L2** is not as likely as reduction of 8^+ as the Lewis acidity of Cu lowers the energy of the frontier orbitals of **L1** and **L2** in addition to the cationic character of 8^+ making that species easier to reduce.

Reduction of 8^{+*} by either **L1** or **L2** was calculated to be unfavorable by 12.6 and 28.3 kcal/mol, respectively, while the reduction of 8^+ by 8^{+*} was nearly thermoneutral at −1.0 kcal/mol. It is thus much more likely that 8^+ is involved in an outer sphere electron transfer event with 8^{+*} than the ligands **L1** or **L2**. This is supported by UV−Vis experiments demonstrating decreased emission above a concentration of 0.1 mM 8^+ upon irradiation by blue light in a solution containing only 8^+ (Figure 8, top). The simplest explanation of this data is the quenching of 8^{+*} by 8^+ disproportionation to 8^{2+} and **8** (Figure 8, bottom). In this context, the primary reducing agent in solution is **8** and the most powerful oxidant is 8^{2+}.

It is worth noting that the concentration of 8^+ in solution is rather high since 10 mol % CuI is used in the reaction with an excess of **L1** and **L2** provided. This puts the concentration of 8^+ and the substrate within an order of magnitude of each other. Therefore, it is cogent to suggest that 8^+ could react with 8^{+*} at the concentrations present if the interaction was favorable.

Electronic Structure of Species 8. The nuclear and electronic structures of **8** are very similar to those of 8^{+*} (Figure 9). Both have a four-coordinate distorted trigonal pyramidal structure, which is expected from a ligand field

https://doi.org/10.1021/acs.inorgchem.1c01038
Inorg. Chem. XXXX, XXX, XXX−XXX

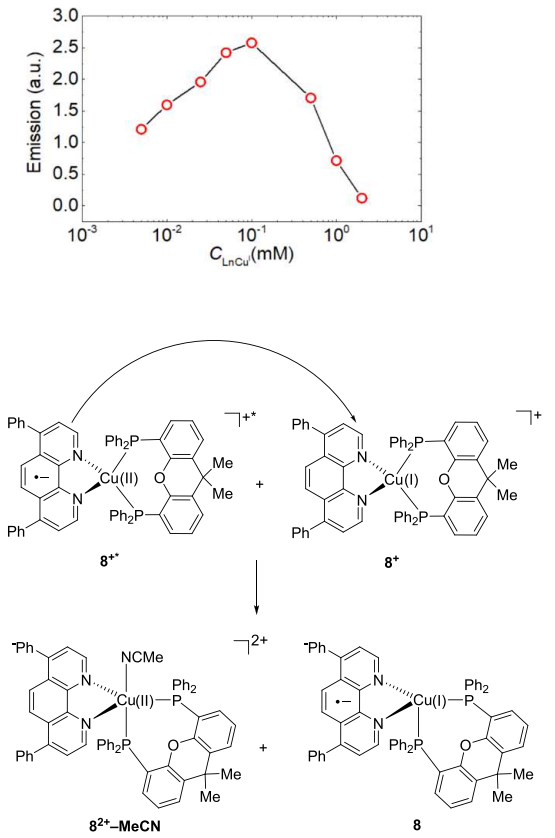

Figure 8. (Top) Emission as a function of chromophore concentration under blue light irradiation. (Bottom) Disproportionation of 8^{+}* and 8^{+} forming **8** and 8^{2+}**–MeCN**.

theory for a d9/d10 metal with two bidentate ligands, one with a wide bite angle (**L1**, 128°) and the other narrower (**L2**, 80°). Both **8** and 8^{+}* have spin density on the **L2** ligand and the Cu center but the Cu spin density is much less pronounced on **8** than 8^{+}*. This is consistent with the identity of the Cu center **2** being a Cu(I) species with a reduced redox active ligand $\mathbf{L2}^{-}$ compared to 8^{+}*, which is a Cu(II) $\mathbf{L2}^{-}$ system.

Outer Sphere Reduction of 12 by 8: Radical Rebound. The prevalence of outer sphere electron transfer mechanisms in the literature of cross-couplings by heteroleptic Cu(I) chromophores necessitates that we examine this possibility in some detail for this system. However, the lack of disruption from intra- and intermolecular radical traps makes a strong argument against the existence of a persistent glycosyl radical species in the dominant mechanism. There is still the possibility that a radical species is generated in the mechanism but binds to a Cu center at a rate greater than the intramolecular radical quenching step. Thus, the feasibility of an outer sphere reduction of **12** to generate **13** was explored (Figure 10).

The reduction of **12** by 8^{+}* has already been demonstrated as unfeasible by experiments and the calculations reported above. However, **8** is more reducing than 8^{+}* so an outer sphere reaction with this species must be investigated. The thermodynamics for such a process are favorable. The outer sphere reduction is −6.2 kcal/mol compared to reactants. For **18** to bind with the coordinatively saturated Cu(I) center, either **L1** or **L2** must dissociate. Radical rebound following the dissociation of **L2** (−14.8 kcal/mol) is more favorable than rebound with the loss of **L1** (−1.4 kcal/mol), but both are favorable compared to reactants (Figure 10). However, the estimated barrier for outer sphere electron transfer is prohibitive enough to warrant investigation into alternate mechanisms.

Using the differences in solvent free energy for reactants and products via non-equilibrium SMD solvation to estimate the intrinsic barrier λ of Marcus theory and calculating the ΔG° from reactants to products allow for estimation of the free energy of electron transfer ΔG^{*} (see SI for details). The barrier for electron transfer from **8** to **12** is estimated at +37.2 kcal/mol (Figure 10), making the process much less facile than thermodynamics alone would suggest. Nevertheless, this result does strongly suggest a physical reason for the observed lack of reactivity between the substrate and radical traps: the barrier for generating free radicals is simply too great to compete with the barriers associated with an inner sphere pathway. To test this assertion, the inner sphere mechanism was evaluated computationally, and the results were compared to the calculated outer sphere reduction parameters.

Possible Oxidative Addition of Pyranosyl Bromide 12 to 8^{+}*. Both TEMPO and an intermolecular alkene group did not react with glycosyl substrates as evidenced by a lack of radical trapping products and an invariance in the yield of the desired product (Scheme 1). Thus, efforts to map out a viable mechanistic pathway computationally were concentrated on an inner sphere oxidative addition/reductive elimination pathway.

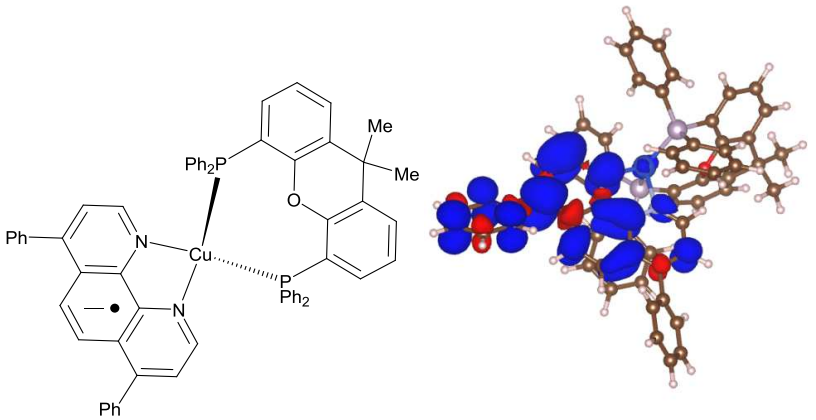

Figure 9. Spin density plot of copper complex **8** showing the major component of spin density located on the phenanthroline ligand **L2** consistent with an $\mathbf{L2}^{-}$ Cu(I) species.

https://doi.org/10.1021/acs.inorgchem.1c01038
Inorg. Chem. XXXX, XXX, XXX−XXX

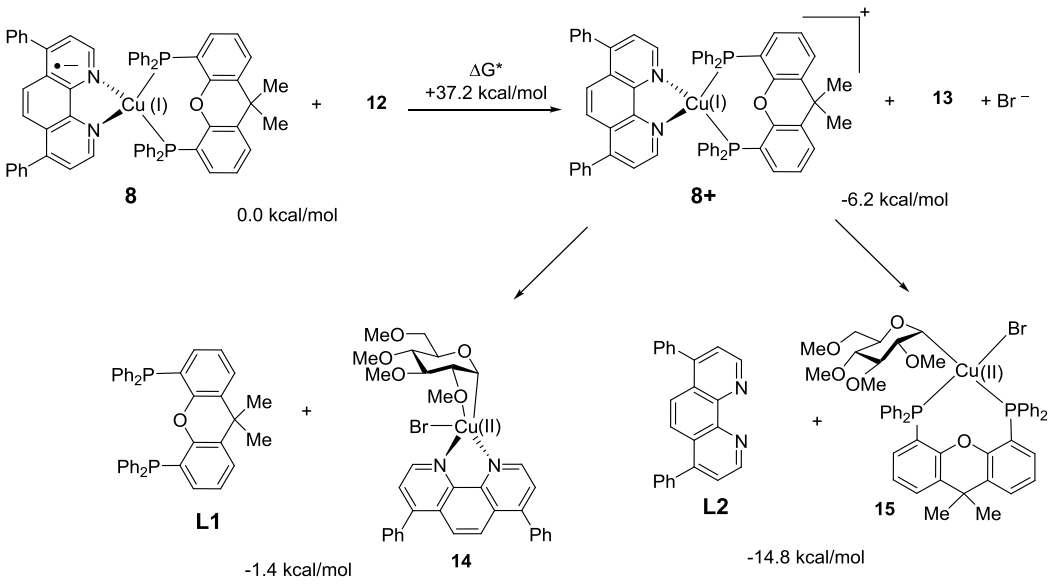

Figure 10. Thermodynamics of outer sphere reduction of **12** by **8** with radical rebound.

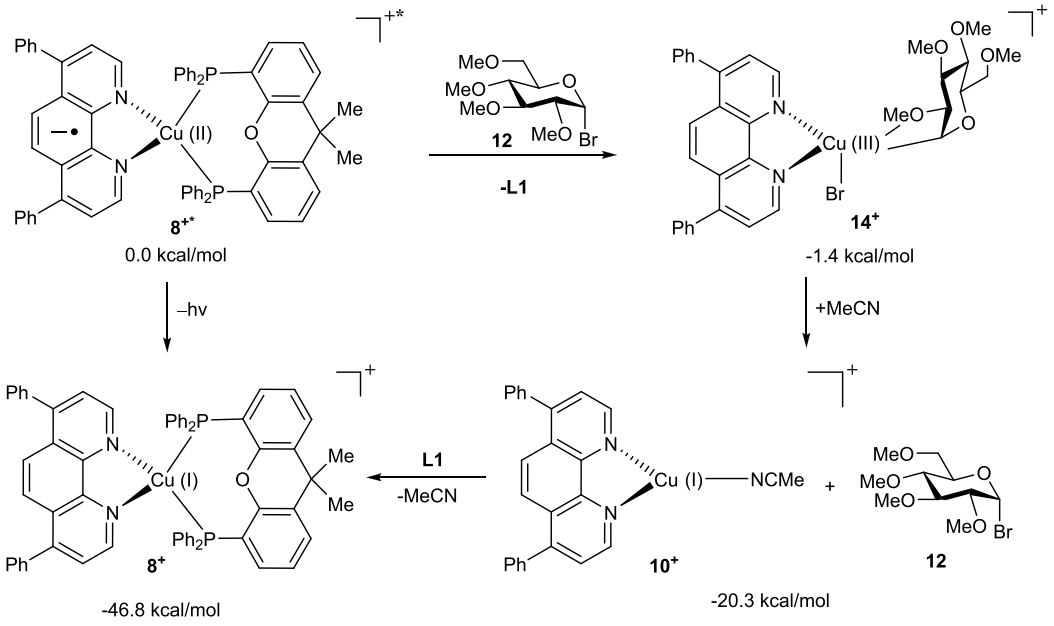

Figure 11. Thermodynamics of nonradiative decay of 8^{+*} by oxidative addition of **12** to 8^{+*}, decomposition of 14^{+} to 10^{+}, and reformation of 8^{+} from 10^{+}.

This study has identified two thermodynamically plausible mechanisms for the activation of substrate **12**: oxidative addition of **12** to 8^{+*} and oxidative addition of **12** to **8** (Figure 11).

While oxidative addition of **12** to 8^{+*} is thermodynamically favorable, there is reason to expect that this process would not be productive in terms of generating products even if it were to occur (Figure 11). Upon oxidative addition of **12** to 8^{+*}, the Cu(III) species 14^{+} is formed. It is well established that Cu(III)−C bonds are generally quite weak and reductive elimination for C-bound species is generally rapid and favorable with few exceptions.[31] This system is not an exception to that rule and reductive elimination from 14^{+} to form the starting materials **12** and 10^{+} is favorable by 18.9 kcal/mol. Additionally, there was a trivially small (∼1 kcal/mol) reaction barrier based on linear synchronous transit probes into the reductive elimination. Thus, there is little prospect of 14^{+} existing for long enough to perform the chemical transformations observed experimentally.

*Oxidative Addition of Pyranosyl Bromide **12** to Copper Complex **8**.* Since the outer sphere electron transfer from **8** to **12** does not fit with experimental observations and the oxidative addition of **12** to 8^{+*} results in a very unstable intermediate, oxidative addition of **12** to **8** was left as the most plausible process and was explored in detail (Figures 12and 13).

Based on electronic structure calculations, **8** is a Cu(I) species with an $L2^{-}$ ligand, indicating decreased Lewis acidity at the metal center and an inversion of the relative binding strength of **L1** and **L2**. The increased Lewis basicity of $L2^{-}$ and the propensity for Cu(I) to form tricoordinate complexes result in a strengthening of Cu−N bonds at the expense of

https://doi.org/10.1021/acs.inorgchem.1c01038
Inorg. Chem. XXXX, XXX, XXX−XXX

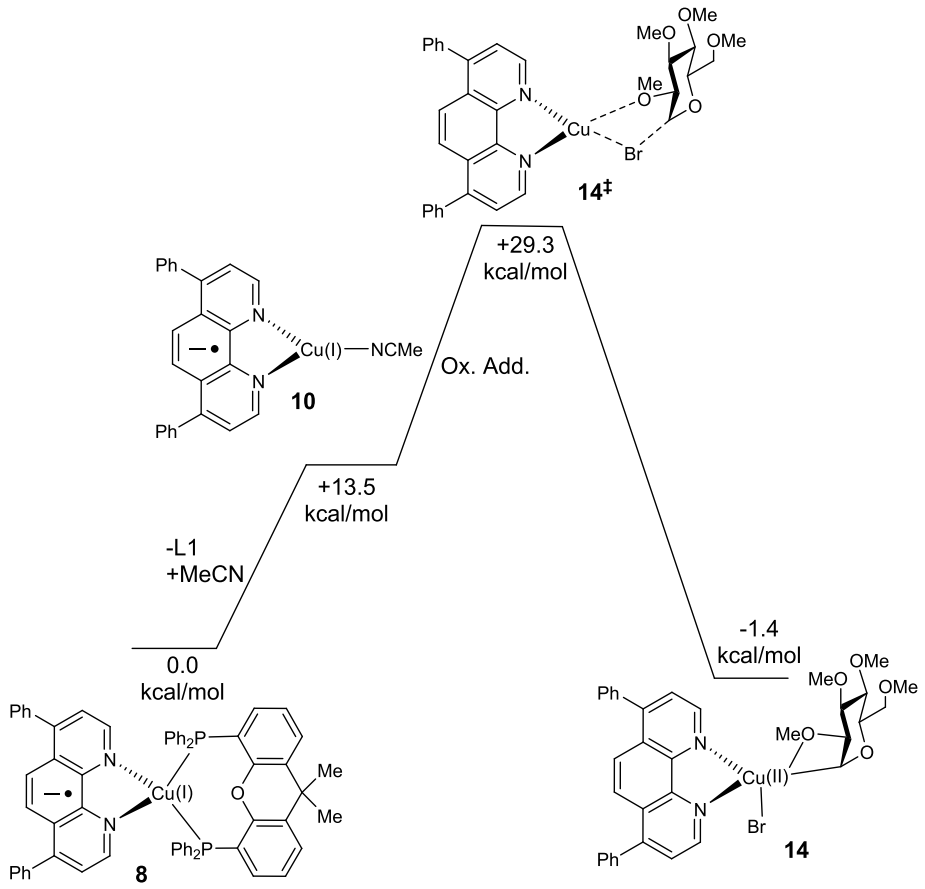

Figure 12. Thermodynamics and kinetic barrier for the formation of **14** from **8** and **10** by stepwise oxidative addition.

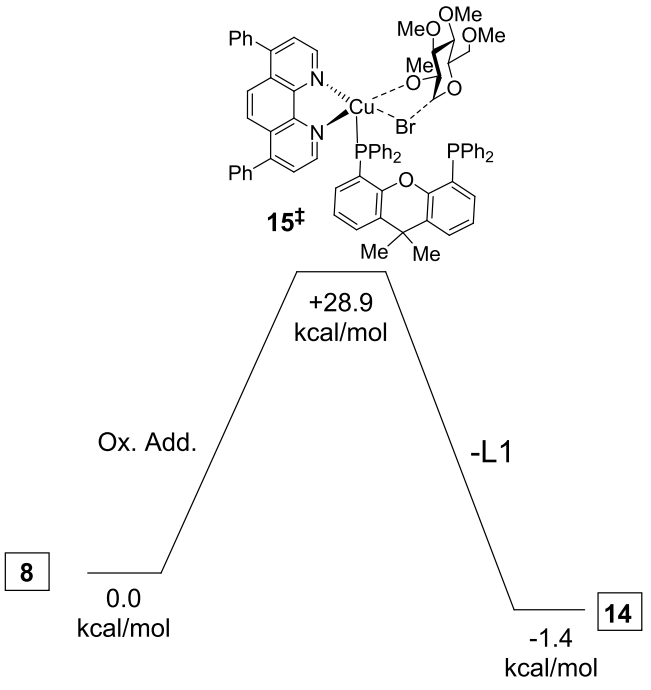

Figure 13. Thermodynamics and kinetic barrier for the formation of **14** from **8** and **12** by concerted oxidative addition.

weakening Cu−P bonds. This effect is observed both by the elongation of Cu−P bonds in **8** compared to $\mathbf{8}^{+}$ and by the much more favorable dissociation of **L1** from **8** than $\mathbf{8}^{+}$. Therefore, while dissociation of **L1** from $\mathbf{2}^{+}$ is very endergonic (+26.4 kcal/mol), the same process is quite accessible from **8** (+13.5 kcal/mol). Once the phosphine ligand dissociates, the resulting species **10** is analogous to phenanthroline ligated copper complexes, which are known to catalyze Ullmann-type coupling under thermally activation as Cu(I) species (Figure 1). As a more electron-rich [Cu(I)($\mathrm{L2}^{-}$)] species, **10** should be able to undergo oxidative addition under milder conditions. Oxidative addition of **9** to **12** proceeds in a facile manner with a barrier of +15.8 kcal/mol for a total barrier of +29.3 kcal/mol starting from **8**. A barrier for concerted oxidative addition of **12** and dissociation of **L1** from **8** was calculated and found to be within the expected computational uncertainty of the stepwise mechanism (Figure 12) at +28.9 kcal/mol. There is little reason to favor either the stepwise (Figure 12) or concerted mechanism (Figure 13) since both mechanisms should be accessible but sluggish at room temperature and are nearly equal in energy.

Formation of Glycosylation Product ***12*** *by Reductive Elimination.* Proceeding from **14** to products is problematic since the Cu(II) configuration of this species is only metastable and oxidation to the Cu(III) species $\mathbf{14}^{+}$ by $\mathbf{8}^{2+}$**−MeCN** is favorable by 18.3 kcal/mol. Upon oxidation to the Cu(III) species $\mathbf{14}^{+}$, reductive elimination producing pyranosyl bromide substrates **12** and $\mathbf{10}^{+}$ is favorable by a further 22.3 kcal/mol with a trivially small barrier (Figure 11). For the desired reaction to compete with the regeneration of starting materials, as observed experimentally, the nucleophilic alcohol **16** should be proximate to the Cu complex so that it can insert into the C1 position before **12** is regenerated (Figure 12). The d9 Cu(II) center of **14** is coordinatively saturated, so binding to

https://doi.org/10.1021/acs.inorgchem.1c01038
Inorg. Chem. XXXX, XXX, XXX−XXX

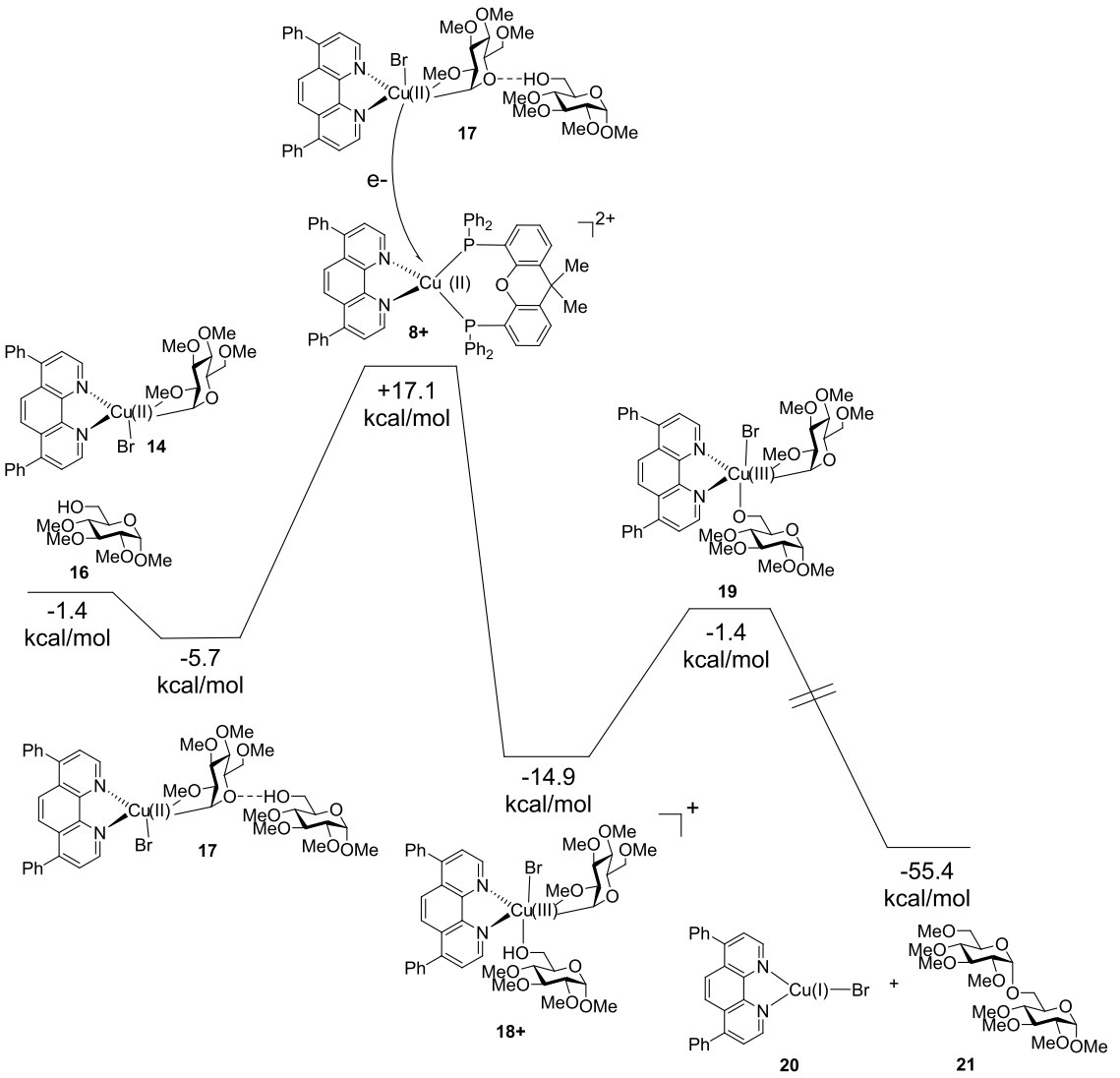

Figure 14. Binding of nucleophilic alcohol **16** to copper complex **14** resulting in the formation of product **21**.

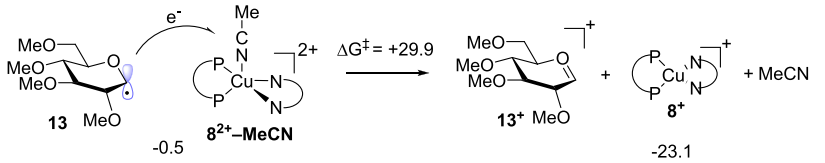

Figure 15. Conversion of glycosyl radical **13** to oxocarbenium $\mathbf{13}^+$ by $\mathbf{8}^{2+}$**–MeCN** through outer sphere electron transfer. Energies are reported in kcal/mol.

the complex is most favorable by bonding between the protic hydrogen of **16** and an ether oxygen of **14** to form the H-bond adduct in complex **17**. This bonding was found to be favorable by 4.3 kcal/mol. Oxidation of **17** to $\mathbf{18}^+$ by $\mathbf{8}^{2+}$**–MeCN** is favorable by 9.2 kcal/mol with an outer electron transfer barrier of +22.8 kcal/mol (Figure 14). This barrier is not high enough for this step to be rate-limiting but it is important since it is high enough to allow for equilibration to occur before oxidation of either **17** or **14** and the resulting reductive elimination. This ensures that there is much more **17** in solution than **14**.

Upon oxidation to $\mathbf{18}^+$, the alcohol **16** is bound to the Cu metal center. Deprotonation of the Cu-bound hydroxyl group of $\mathbf{18}^+$ by DTBMP to form **19** is accessible at +13.5 kcal/mol and leads to the reductive elimination to produce the desired product **21** and the intermediate **20**, which is very favorable at −54.0 kcal/mol. The LST detected barrier from **19** to **21** is trivially small so it is likely that the deprotonation and product formation proceed in a concerted fashion. Free **L1** can then displace the Br^- species of **20** to regenerate $\mathbf{8}^+$ and reset the cycle.

Possible Side Reaction by Radical Dissociation. The calculated electronic structure of **14** places a significant radical character between the glycoside C1 and Cu, indicating a weakened bond. The free energy of dissociation generating glycosyl radical **13** from **14** is calculated to be unfavorable by only +0.9 kcal/mol. The magnitude of this energy difference suggests a significant Boltzmann distribution of **13** and **14**

https://doi.org/10.1021/acs.inorgchem.1c01038
Inorg. Chem. XXXX, XXX, XXX−XXX

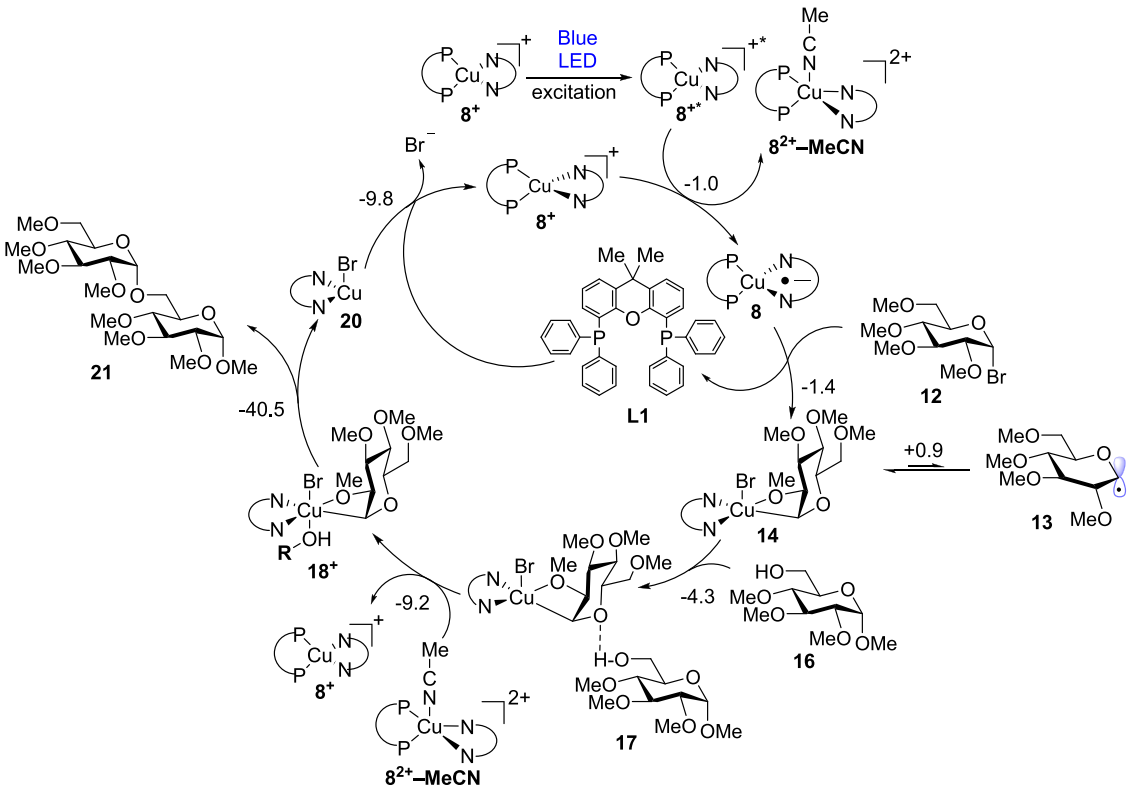

Figure 16. Overview of the inner sphere mechanism.

existing in solution with the equilibrium favoring **14**. The calculations are not expected to have the degree of accuracy to predict the distribution of **14** to **13** precisely, but the calculated range is on the order of 10:1. Oxidation of **13** by $\mathbf{8^{2+}}$**–MeCN** is favorable by −23.1 kcal/mol, forming the oxocarbenium $\mathbf{13^+}$. The calculated barrier for outer sphere electron transfer is 29.9 kcal/mol including the radical dissociation step. This puts this pathway on an even footing with the inner sphere mechanism (Figure 15). The relatively high barrier for SET can be attributed to the large solvation reorganization involved in the electron transfer process.

Nucleophilic attack by the alcohol **16** on the carbocationic C1 to form $\mathbf{21\text{-}H^+}$ is exergonic by 11.6 kcal/mol and is not expected to be anomerically selective due to the planarity of the C1 carbon environment of $\mathbf{8^+}$. Deprotonation of $\mathbf{21\text{-}H^+}$ to **21** by DTBMP is also expected to be facile at −33.6 kcal/mol. Accepting that the equilibrium of **14** to **13** is ∼10:1 and the conversion of **13** to a 1:1 mixture of **21** is competitive to inner sphere, this gives us a product distribution of approximately 20:1, which is reasonably close to the observed 93:7 distribution observed experimentally.

Overview of the Inner Sphere Mechanism. Figure 16 illustrates the overall mechanism of visible light-mediated photoinduced copper-catalyzed cross-coupling of pyranosyl bromide with aliphatic alcohol based on our calculations. The most viable target for reduction by $\mathbf{8^{+}*}$ was found to be $\mathbf{8^+}$, resulting in a disproportionation reaction producing **8** and $\mathbf{8^{2+}}$**–MeCN**. Formation of **14** by oxidative addition of the pyranosyl bromide **12** to **8** can proceed by either a concerted mechanism displacing **L1** while **8** undergoes oxidative addition ($\Delta G^{\ddagger}$ = +29.3 kcal/mol) or by a stepwise mechanism with the dissociation of **L1** followed by oxidative addition of **12** ($\Delta G^{\ddagger}$ = +28.9 kcal/mol). The oxidative addition step is calculated to be exergonic, making the forward reaction generating **14** significantly faster than the backward reaction.

To proceed to the reductive elimination of products from Cu, the metal center must be oxidized to a Cu(III) state. The instability of Cu(III)−C bonds necessitates that the nucleophilic substrate be in the coordination sphere of the complex to be able to compete with the unproductive reductive elimination of starting substrates. Since the Cu center of **14** is already coordinatively saturated, the H-bonding of alcohol nucleophiles **16** and **14** to produce species **17** was probed and found to be exergonic by 4.3 kcal/mol. Favorable oxidation of **17** by $\mathbf{8^{2+}}$**–MeCN** yields $\mathbf{18^+}$ and coordination of the nucleophilic alcohol **16** at the primary coordination sphere of the Cu(III) center. Deprotonation of **18** allows for the reductive elimination of **21** from $\mathbf{18^+}$, leaving the Cu−Br species **20**. Displacement of Br^- from **20** by **L1** regenerates $\mathbf{8^+}$ and resets the cycle.

CONCLUSIONS

A plausible mechanism for the anomerically specific copper-catalyzed cross-coupling of pyranosyl bromides with aliphatic alcohols has been deduced by experimental and theoretical investigation. Electrochemical and spectrochemical experiments and detailed computational studies confirmed that the activated chromophore $\mathbf{8^{+}*}$ was not capable of directly reducing a bromoglucoside to a glycosyl radical. Examining the other species in solution, it was determined that the most likely species for $\mathbf{8^{+}*}$ to reduce was, to our surprise, $\mathbf{8^+}$. The resulting disproportionation reaction producing $\mathbf{8^{2+}}$**–MeCN** and **8** was found to be favorable by 1 kcal/mol (Figure 8).

Drawing inspiration from the literature,[28] we evaluated **8** as a reductant and found that it was stronger than the excited chromophore $\mathbf{8^{+}*}$. The thermodynamics for outer sphere

https://doi.org/10.1021/acs.inorgchem.1c01038
Inorg. Chem. XXXX, XXX, XXX−XXX

reduction of **12** by **8** are favorable. However, experimentally, the reaction was not inhibited by the presence of inter- and intramolecular radical traps (Scheme 1), indicating that generation of a free radical species was unlikely. Calculating the electron transfer barrier for transferring an electron from **8** within Marcus theory revealed that the formation of a glycosyl radical was prevented by a large reorganization energy, leading to a prohibitively high electron transfer barrier (+37.2 kcal/mol) (Figure 10).

An inner sphere mechanism was explored and found to be more favorable than the free radical pathway. The inner sphere pathway can proceed by either a stepwise dissociation of **L1** followed by oxidative addition of carbohydrate substrate **12** ($\Delta G^{\ddagger}$ = +29.3 kcal/mol) (Figure 12) or a concerted oxidative addition/dissociation step ($\Delta G^{\ddagger}$ = +28.9 kcal/mol) (Figure 13). From the stepwise process, we deduce that the dissociation of **L1** from **8** accounts for ∼13.5 kcal/mol of this barrier and the oxidative addition of **12** contributes ∼15.8 kcal/mol. The resulting intermediate, **14**, was oxidized readily by the **8**$^{2+}$**−MeCN** but the calculated barrier for outer sphere oxidation of **8** is +22.8 kcal/mol so it is reasonable to expect a degree of metastability for this species.

The electronic structure of **14** has significant spin on the C1 position of the Cu-bound glycoside, indicating a radical character for that species. Dissociation of the glycosyl radical **13** from **14** is calculated to be unfavorable by 0.9 kcal/mol (Figure 15). However, for **14** to react with the alcohol **16**, it must be oxidized to the carbocationic species **14**$^{+}$ by **8**$^{2+}$**−MeCN**, which has a barrier of +29.9 kcal/mol. This makes the outer sphere process slower than the inner sphere mechanism ($\Delta G^{\ddagger}$ = +28.9 kcal/mol). It is also possible that the model used here to evaluate entropy significantly overestimates the free energy of glycosyl radical **13** in solution and thus is biased to predict dissociation from Cu. The observed inactivity of radical traps favors the latter explanation, but the generation of equatorially β-linked side products can be explained by the former.

Hydrogen bonding of the nucleophilic alcohol **16** to **14** to form **17** is favorable by −4.3 kcal/mol and places **16** in a favorable position to attach to Cu upon oxidation of **17** (Figure 14). If this were not the case, then reductive elimination to form starting materials would be likely owing to the well-known instability of Cu(III)−C bonds.

Oxidation of **17** to **8**$^{2+}$**−MeCN** forming the species **18**$^{+}$ is favorable by −9.2 kcal/mol (Figure 14) and places **16** in the primary coordination sphere. Upon oxidation to a Cu(III) species, reductive elimination to form products is expected to be rapid due to the lack of a significant barrier for product formation. Deprotonation of the protic hydrogen of **18**$^{+}$ by DTBMP followed by rapid reductive elimination form the product **21**. Displacement of Br from the intermediate species **20** by free **L1** regenerates **8**$^{+}$ and resets the cycle.

This cross-coupling protocol enables highly diastereoselective access to the challenging axial 1,2-glycosides, important motifs found in a variety of bioactive carbohydrate molecules.[32−36] Our mechanistic studies provide a foundation for developing novel carbohydrate methods to stereoselective construction of natural and unnatural anomeric carbon(sp^3)−heteroatom glycosidic bonds as well as anomeric carbon(sp^3)−carbon linkages.

■ ASSOCIATED CONTENT

Supporting Information

The Supporting Information is available free of charge at https://pubs.acs.org/doi/10.1021/acs.inorgchem.1c01038.

Computational details; calculating electron transfer barriers with non-equilibrium solvation models and Marcus theory; UV−Vis and emission spectra of relevant copper complexes; calculated homoleptic Cu complexes of **L1** and **L2**; and Cartesian coordinates and free energies of calculated species (PDF)

■ AUTHOR INFORMATION

Corresponding Authors

Hien M. Nguyen − *Department of Chemistry, Wayne State University, Detroit, Michigan 48202, United States*; Email: hmnguyen@wayne.edu

H. Bernhard Schlegel − *Department of Chemistry, Wayne State University, Detroit, Michigan 48202, United States*; orcid.org/0000-0001-7114-2821; Email: hbs@chem.wayne.edu

Author

Richard N. Schaugaard − *Department of Chemistry, Wayne State University, Detroit, Michigan 48202, United States*; orcid.org/0000-0003-3351-8810

Complete contact information is available at: https://pubs.acs.org/10.1021/acs.inorgchem.1c01038

Notes

The authors declare no competing financial interest.

■ ACKNOWLEDGMENTS

This research is supported by NIH (U01GM120293 for H.M.N.) and NSF (CHE1856437 for H.B.S.). We thank the Wayne State University Grid for computing resources.

■ REFERENCES

(1) Ullmann, F.; Bielecki, J. Ueber Synthesen in der Biphenylreihe. *Ber. Dtsch. Chem. Ges.* **1901**, *34*, 2174−2185.

(2) Ullmann, F. Ueber eine neue Bildungsweise von Diphenylaminderivaten. *Ber. Dtsch. Chem. Ges.* **1903**, *36*, 2382−2384.

(3) Ullmann, F.; Sponagel, P. Ueber die Phenylirung von Phenolen. *Ber. Dtsch. Chem. Ges.* **1905**, *38*, 2211−2212.

(4) Goldberg, I. Ueber Phenylirungen bei Gegenwart von Kupfer als Katalysator. *Ber. Dtsch. Chem. Ges.* **1906**, *39*, 1691−1692.

(5) Yeung, C. S.; Dong, V. M. Catalytic Dehydrogenative Cross-Coupling: Forming Carbon−Carbon Bonds by Oxidizing Two Carbon−Hydrogen Bonds. *Chem. Rev.* **2011**, *111*, 1215−1292.

(6) Johansson Seechurn, C. C. C.; Kitching, M. O.; Colacot, T. J.; Snieckus, V. Palladium-Catalyzed Cross-Coupling: A Historical Contextual Perspective to the 2010 Nobel Prize. *Angew. Chem., Int. Ed.* **2012**, *51*, 5062−5085.

(7) Beletskaya, I. P.; Cheprakov, A. V. The Heck Reaction as a Sharpening Stone of Palladium Catalysis. *Chem. Rev.* **2000**, *100*, 3009.

(8) Sawatzky, R. S.; Hargreaves, B. K. V.; Stradiotto, M. A Comparative Ancillary Ligand Survey in Palladium-Catalyzed C−O Cross-Coupling of Primary and Secondary Aliphatic Alcohols. *Eur. J. Org. Chem.* **2016**, *2016*, 2444−2449.

(9) Ruiz-Castillo, P.; Buchwald, S. L. Applications of Palladium-Catalyzed C−N Cross-Coupling Reactions. *Chem. Rev.* **2016**, *116*, 12564−12649.

(10) Dorel, R.; Grugel, C. P.; Haydl, A. M. The Buchwald−Hartwig Amination After 25 Years. *Angew. Chem., Int. Ed.* **2019**, *58*, 17118−17129.

(11) Hossain, A.; Bhattacharyya, A.; Reiser, O. Copper's rapid ascent in visible-light photoredox catalysis. *Science* **2019**, *364*, eaav9713.
(12) Bhunia, S.; Pawar, G. G.; Kumar, S. V.; Jiang, Y.; Ma, D. Selected Copper-Based Reactions for C−N, C−O, C−S, and C−C Bond Formation. *Angew. Chem., Int. Ed.* **2017**, *56*, 16136−16179.
(13) Beletskaya, I. P.; Cheprakov, A. V. Copper in Cross-Coupling Reactions: The Post-Ullmann Chemistry. *Coord. Chem. Rev.* **2004**, *248*, 2337.
(14) Monnier, F.; Taillfer, M. Catalytic C-C, C-N, and C-O Ullmann-Type Coupling Reactions. *Angew. Chem., Int. Ed.* **2009**, *48*, 6954.
(15) Chan, D. M. T.; Monaco, K. L.; Wang, R.-P.; Winters, M. P. New N- and O-arylations with phenylboronic acids and cupric acetate. *Tetrahedron Lett.* **1998**, *39*, 2933−2936.
(16) Evans, D. A.; Katz, J. L.; West, T. R. Synthesis of diaryl ethers through the copper-promoted arylation of phenols with arylboronic acids. An expedient synthesis of thyroxine. *Tetrahedron Lett.* **1998**, *39*, 2937−2940.
(17) Sambiagio, C.; Marsden, S. P.; Blacker, A. J.; McGowan, P. C. Copper catalysed Ullmann type chemistry: from mechanistic aspects to modern development. *Chem. Soc. Rev.* **2014**, *43*, 3525−3550.
(18) Jones, G. O.; Liu, P.; Houk, K. N.; Buchwald, S. L. Computational Explorations of Mechanisms and Ligand-Directed Selectivities of Copper-Catalyzed Ullmann-Type Reactions. *J. Am. Chem. Soc.* **2010**, *132*, 6205.
(19) McMillin, D. R.; Buckner, M. T.; Ahn, B. T. A light-induced redox reaction of bis(2,9-dimethyl-1,10-phenanthroline)copper(I). *Inorg. Chem.* **1977**, *16*, 943−945.
(20) Kern, J.-M.; Sauvage, J.-P. Photoassisted C−C coupling via electron transfer to benzylic halides by a bis(di-imine) copper(I) complex. *J. Chem. Soc., Chem. Commun.* **1987**, *8*, 546−548.
(21) Creutz, S. E.; Lotito, K. J.; Fu, G. C.; Peters, J. C. Photoinduced Ullmann C−N Coupling: Demonstrating the Viability of a Radical Pathway. *Science* **2012**, *338*, 647−651.
(22) Bissember, A. C.; Lundgren, R. J.; Creutz, S. E.; Peters, J. C.; Fu, G. C. Transition-Metal-Catalyzed Alkylations of Amines with Alkyl Halides: Photoinduced, Copper-Catalyzed Couplings of Carbazoles. *Angew. Chem., Int. Ed.* **2013**, *52*, 5129−5133.
(23) Uyeda, C.; Tan, Y.; Fu, G. C.; Peters, J. C. A New Family of Nucleophiles for Photoinduced, Copper-Catalyzed Cross-Couplings via Single-Electron Transfer: Reactions of Thiols with Aryl Halides Under Mild Conditions (O °C). *J. Am. Chem. Soc.* **2013**, *135*, 9548−9552.
(24) Matier, C. D.; Schwaben, J.; Peters, J. C.; Fu, G. C. Copper-Catalyzed Alkylation of Aliphatic Amines Induced by Visible Light. *J. Am. Chem. Soc.* **2017**, *139*, 17707−17710.
(25) Yu, F.; Dickson, J. L.; Loka, R. S.; Xu, H.; Schaugaard, R. N.; Schlegel, H. B.; Luo, L.; Nguyen, H. M. Diastereoselective sp3 C−O Bond Formation via Visible Light-Induced, Copper-Catalyzed Cross-Couplings of Glycosyl Bromides with Aliphatic Alcohols. *ACS Catal.* **2020**, *10*, 5990−6001.
(26) Bagal, D. B.; Kachkovskyi, G.; Knorn, M.; Rawner, T.; Bhanage, B. M.; Reiser, O. Trifluoromethylchlorosulfonylation of Alkenes: Evidence for an Inner-Sphere Mechanism by a Copper Phenanthroline Photoredox Catalyst. *Angew. Chem., Int. Ed.* **2015**, *54*, 6999.
(27) Rawner, T.; Lutsker, E.; Kaiser, C. A.; Reiser, O. The Different Faces of Photoredox Catalysts: Visible-Light-Mediated Atom Transfer Radical Addition (ATRA) Reactions of Perfluoroalkyl Iodides with Styrenes and Phenylacetylenes. *ACS Catal.* **2018**, *8*, 3950−3956.
(28) Michelet, B.; Deldaele, C.; Kajouj, S.; Moucheron, C.; Evano, G. A General Copper Catalyst for Photoredox Transformations of Organic Halides. *Org. Lett.* **2017**, *19*, 3576−3579.
(29) Beniazza, R.; Molton, F.; Duboc, C.; Tron, A.; McClenaghan, N. D.; Lastecoueres, D.; Vincent, J. M. Copper(I)-photocatalyzed trifluoromethylation of alkenes. *Chem. Commun.* **2015**, *51*, 9571.
(30) Le, C.; Chen, T. Q.; Liang, T.; Zhang, P.; MacMillan, D. W. C. A radical approach to the copper oxidative addition problem: Trifluoromethylation of bromoarenes. *Science* **2018**, *360*, 1010−1014.
(31) Paeth, M.; Tyndall, S. B.; Chen, L.-Y.; Hong, J.-C.; Carson, W. P.; Liu, X.; Sun, X.; Liu, J.; Yang, K.; Hale, E. M.; Tierney, D. L.; Liu, B.; Cao, Z.; Cheng, M.-J.; Goddard, W. A.; Liu, W. Csp3−Csp3 Bond-Forming Reductive Elimination from Well-Defined Copper(III) Complexes. *J. Am. Chem. Soc.* **2019**, *141*, 3153−3159.
(32) Nigudkar, S. S.; Demchenko, A. V. Stereocontrolled 1,2-Cis Glycosylation As the Driving Force of Progress in Synthetic Carbohydrate Chemistry. *Chem. Sci.* **2015**, *6*, 2687.
(33) Mensah, E. A.; Nguyen, H. M. Nickel-Catalyzed Stereoselective Formation of α-2-Deoxy-2-Amino Glycosides. *J. Am. Chem. Soc.* **2009**, *131*, 8778.
(34) Mensah, E. A.; Yu, F.; Nguyen, H. M. Nickel-Catalyzed Stereoselective Glycosylation with C(2)-N-Substituted Benzylidene D-Glucosamine and Galactosamine Trichloroacetimidates for the Formation of 1,2-Cis-2-Amino Glycosides. Applications to the Synthesis of Heparin Disaccharides, GPI Anchor Psuedodisaccharides, and α-GalNAc. *J. Am. Chem. Soc.* **2010**, *132*, 14288.
(35) Evano, G.; Blanchard, N.; Toumi, M. Copper-Mediated Coupling Reactions and Their Applications in Natural Products and Designed Biomolecules Synthesis. *Chem. Rev.* **2008**, *108*, 3054.
(36) Allen, S. E.; Walvoord, R. R.; Padilla-Salinas, R.; Kozlowski, M. C. Aerobic Copper-Catalyzed Organic Reactions. *Chem. Rev.* **2013**, *113*, 6234.

https://doi.org/10.1021/acs.inorgchem.1c01038
Inorg. Chem. XXXX, XXX, XXX−XXX